NSF (Grant No. CHE 8509325). This work was funded in part by an additional grant from 3M.

Registry No. Cr(2,6-diisopropylphenyl isocyanide)$_6$, 61770-86-3; Cr(2,6-diisopropylphenyl isocyanide)$_6^+$, 82456-69-7; Cr(2,6-diisopropylphenyl isocyanide)$_6^{2+}$, 82456-70-0; Cr(2,6-diisopropylphenyl isocyanide)$_6^{3+}$, 82456-71-1; Cr(2,6-dimethylphenyl isocyanide), 82456-65-3; Cr(2,6-dimethylphenyl isocyanide)$^+$, 82456-66-4; Cr(2,6-dimethylphenyl isocyanide)$^{2+}$, 82456-67-5; Cr(2,6-dimethylphenyl isocyanide)$^{3+}$, 82456-68-6; Cr(2-methylphenyl isocyanide), 57016-37-2; Cr(2-methylphenyl isocyanide)$^+$, 57016-38-3; Cr(2-methylphenyl isocyanide)$^{2+}$, 57016-40-7; Cr(2-methylphenyl isocyanide)$^{3+}$, 82469-01-0; Cr(phenyl isocyanide), 17375-15-4; Cr(phenyl isocyanide)$^+$, 57016-32-7; Cr(phenyl isocyanide)$^{2+}$, 57016-35-0; Cr(phenyl isocyanide)$^{3+}$, 70801-01-3; Cr(4-chlorophenyl isocyanide), 36732-52-2; Cr(4-chlorophenyl isocyanide)$^+$, 57016-50-9; Cr(4-chlorophenyl isocyanide)$^{2+}$, 57016-52-1; Cr(4-chlorophenyl isocyanide)$^{3+}$, 82456-73-3.

Supplementary Material Available: Plots of IR spectroelectrochemical data for each oxidation of all complexes and UV–vis spectroelectrochemical data for all oxidations involving nonphotosensitive complexes, UV–vis spectra of all oxidation states of each complex studied, and illustrations of the electrode arrangement (24 pages). Ordering information is given on any current masthead page.

Contribution from the Department of Chemistry, Wayne State University, Detroit, Michigan 48202

Stereochemical Inhibition of Substitution in Simple Coordination Compounds. Experimental and Molecular Mechanics Evidence for Discrimination between Dissociative and Interchange Pathways in *trans*-Dichloro(*meso*- and *rac*-(*1,8*)-5,7,7,12,14,14-hexamethyl-1,4,8,11-tetraazacyclotetradeca-4,11-diene)cobalt-(III)[1]

Carolyn L. Schwarz and John F. Endicott*

Received August 15, 1988

High-field ^{1}H NMR studies have shown that acid hydrolysis of the title complex gave a nonequilibrium mixture of aquo–chloro complexes when the macrocyclic ligand was in the racemic conformation. The cobalt center of this complex, Co(*rac*-(*N*)-Me$_6$-[14]dieneN$_4$)Cl$_2^+$, has two different sites for substitution: one protected by axial geminal methyl and other functional groups of the macrocyclic ligand and one relatively unrestricted. The least favored aquo–chloro isomer could not be detected in equilibrated solutions, indicating that the substitution of water for chloride at the most congested site is thermodynamically favored by a factor of at least 10^2. Molecular mechanics calculations are in agreement with this thermodynamic selectivity. However, the thermodynamically least stable isomer is a major initial aquation product, and approximately equal amounts of the two chloro–aquo isomers were found to result from the first aquation of Co(*rac*-(*N*)-Me$_6$[14]dieneN$_4$)Cl$_2^+$. That substitution at the relatively uncongested site is kinetically, but not thermodynamically, favored implicates an interchange mechanism in which stereochemical protection of the coordination site from the entering water molecule countervails the stereochemical (macrocyclic ligand–Cl) repulsions that weaken the Co–Cl bond at this site. Such stereochemical protection of the coordination site is implied in the molecular mechanics calculations, which show that the weaker Co–Cl bond must be stretched more than 1.5 Å before the leaving group is free from the influence of the geminal methyl and other groups near the stereochemically congested site. The observations on several systems are in accord with a prevailing interchange mechanism for substitution, but with the interchange of ligands becoming increasingly dissociative as the substitution site becomes more congested.

Introduction

Ligand substitution reactions in cobalt(III) complexes have been so thoroughly investigated over the past 30 years[2,3] that their kinetic behavior has been described as paradigmatic of the dissociative interchange mechanism.[3b] This mechanistic assignment was in part based on the direct proportionality observed between the rate and equilibrium constants for Co(III) hydrolyses,[3] and it has been reasonably well supported by the small positive values found for volumes of activation.[4,5] Nevertheless, there are some peculiar features of the rate behavior in certain classes of cobalt(III) complexes, and different mechanistic pathways for substitution have sometimes been proposed. Most notably, there has been an almost universal postulation of a dissociative pathway for substitution in *trans*-Co^{III}(N$_4$)XY complexes in which the equatorial ligand is a tetraaza macrocycle.[6-9] Poon's work[6] has been especially systematic in its attempt to assess the effects of (a) the stereochemistry of alkyl substituents on the macrocyclic

(1) Acknowlegement is made to the donors of the Petroleum Research Fund, administered by the American Chemical Society, for the partial support of this research.

(2) Basolo, F.; Pearson, R. G. *Mechanisms of Inorganic Reactions*; Wiley: New York, 1968.
(3) (a) Langford, C. H.; Gray, H. B. *Ligand Substitution Processes*; W. A. Benjamin: New York, 1965. (b) Langford, C. H.; Sastri, V. S. In *M. T. P. Reviews of Science*; Tobe, M. L., Ed.; Butterworths: London, 1972; Vol. 9, Series 2, p 203.
(4) Swaddle, T. W. In *Mechanistic Aspects of Inorganic Reactions*; Rorabacher, D. B., Endicott, J. F., Eds.; ACS Symposium Series 198; American Chemical Society: Washington, DC, 1982.
(5) Palmer, A.; Kelm, H. *Coord. Chem. Rev.* **1981**, *36*, 89.
(6) (a) Poon, C.-K.; Lau, T.-C. L.; Kan, Y.-P. *J. Chem. Soc., Dalton Trans* **1983**, 1641. (b) Poon, C.-K.; Liaso, Sarah S. T. *J. Chem. Soc., Dalton Trans.* **1978**, 1180. (c) Poon, C.-K.; Mak, P.-W. *J. Chem. Soc., Dalton Trans* **1978**, 216. (d) Poon, C.-K.; Wong, C.-L.; Make, P.-W. *J. Chem. Soc., Dalton Trans.* **1977**, 1931. (e) Poon, C.-K.; Wan, W.-K.; Liaso, Sarah S. T. *J. Chem. Soc., Dalton Trans.* **1977**, 1247. (f) Poon, C.-K.; Wong, C.-L. *J. Chem. Soc., Dalton Trans.* **1977**, 523. (g) Poon, C.-K.; Wong, C.-L. *J. Chem. Soc., Dalton Trans.* **1976**, 966. (h) Chau, W.-K.; Lee, W. K.; Poon, C.-K. *J. Chem. Soc., Dalton Trans.* **1974**, 2419. (i) Poon, C.-K.; Tong, H.-W. *J. Chem. Soc., Dalton Trans.* **1974**, 930. (j) Poon, C.-K.; Tong, H.-W. *J. Chem. Soc., Dalton Trans.* **1974**, 1. (k) Poon, C.-K.; Tong, H.-W. *J. Chem. Soc., Dalton Trans.* **1973**, 1301. (l) Mak, P.-W.; Poon, C.-K.; *Inorg. Chem.* **1976**, *15*, 1949. (m) Poon, C.-K. *Proc. Int. Conf. Coord. Chem., XVI* **1974**, 3.47. (n) Lai, T. F.; Poon, C-K. *Inorg. Chem.* **1976**, *15*, 1562. (o) Poon, C.-K.; Wong, C.-L. *Inorg. Chem.* **1976**, *15*, 1562. (p) Poon, C.-K.; Wong, C.-L. *Inorg. Chem.* **1976**, *15*, 1573. (q) Lee, W.-K.; Poon, C.-K. *Inorg. Chem.* **1974**, *12*, 2016. (r) Poon, C.-K. *Coord. Chem. Rev.* **1973**, *10*, 1. (s) Mok, K.-S.; Poon, C.-K.; Tong, H.-W. *J. Chem. Soc. Dalton Trans.* **1972**, 1701. (t) Lui, C.-K.; Poon, C.-K. *J. Chem. Soc., Dalton Trans.* **1972**, 216. (u) Mok, K.-S.; Poon, C.-K. *J. Chem. Soc., Dalton Trans.* **1971**, 1358. (v) Poon, C.-K. *Inorg. Chim. Acta* **1971**, 2151. (w) Chau, W.-K.; Poon, C.-K. *J. Chem. Soc. A* **1971**, 3087. (x) Poon, C.-K.; Tong, H.-W. *J. Chem. Soc. A* **1971**, 2151. (y) Poon, C.-K. *Inorg. Chim. Acta Rev.* **1970**, *4*, 123. (z) Poon, C.-K.; Mok, K.-S. *Inorg. Chem.* **1971**, *10*, 225. (aa) Poon, C.-K.; Mok, K.-S. *J. Am. Chem. Soc.* **1970**, *92*, 4467. (bb) Poon, C.-K.; Tobe, M. L. *Inorg. Chem.* **1968**, *7*, 2398. (cc) Poon, C.-K.; Tobe, M. L. *Inorg. Chem.* **1968**, 1549. (dd) Poon, C.-K.; Tobe, M. L. *Chem. Commun.* **1968**, *3*, 156. (ee) Poon, C.-K.; Tobe, M. L. *J. Chem. Soc. A* **1967**, 2069. (ff) Bosnich, B.; Poon, C.-K.; Tobe, M. L. *Inorg. Chem.* **1965**, *4*, 1102.

0020-1669/89/1328-4011$01.50/0

ligand, (b) the ring size and ring strain, (c) the configuration of chiral nitrogen donors of the macrocycle, and (d) the degree of unsaturation of the macrocycle. The assignment of a dissociative pathway in these systems has been based on accumulated kinetic evidence, the most important of which is considered to be that (a) reaction rates vary as the leaving group is changed (while no other ligands are changed) and (b) steric crowding of the reaction site tends to accelerate the rate (since stereochemical repulsions can often be relaxed by passing to a transition state of lower coordination number). For example, Hay et al. report that the acid hydrolysis rate consts. of the two axially different isomers[10,11] of *trans*-Co(*rac*-(*N*)-Me_6[14]dieneN$_4$)$(NO_2)Cl^+$ [11] are 4.8×10^{-4} [7] and 0.1 s^{-1},[6p] respectively, for Cl^- leaving the stereochemically uncongested and congested coordination sites. This difference in the reactivity of the "open" and "congested" (by axial geminal methyl groups) sites was rationalized in terms of the macrocycle's ability to fold in the transition state, thus labilizing the chloride in the congested site. This interpretation ignores any contributions to the substitution rate from the differences in the complex stabilities, and thus seems potentially inconsistent with much of the earlier work on Co(III) substitutions.

The relationship between structure, reactivity, and strain energy has long been recognized, but it has generally been difficult to quantify for transition-metal complexes.[12] One approach to this problem is to simulate the strain energy changes along the reaction coordinate by using molecular mechanics methods. Hung and Busch[8] have found that ground-state strain energies coorelate well with Cl^- aquation rates in a homologous series of *trans*-Co(N$_4$)Cl_2^+ complexes with aliphatic, unsubstituted macrocyclic ligands (N$_4$ = [14]aneN$_4$–[16]aneN$_4$). Brubaker and Johnson[9] have modeled the dissociative limit for this series of complexes in order to establish that the differences in strain energy between the 5-coordinate intermediate and the ground state do correlate with the trend in substitution rates. An unstated assumption of these analyses is that the equilibrium constants for the overall hydrolyses either are invariant, are not correlated to the hydrolysis rates, or vary in direct proportion to variations in transition-state stability.

We were led to reexamine some of these issues by our observation that replacement of water in the sterically congested site of *trans*-[Pri-CH_3]-Co(*rac*-(*N*)-Me_6[14]dieneN$_4$)$(OH_2)CH_3^{2+}$ [11] (see Figure 1) was several hundred times slower than the very similar substitutions at stereochemically uncongested axial sites of complexes such as *trans*-Co([14]aneN$_4$)$(OH_2)CH_3^{2+}$.[11,13] The significance of this contrast in reactivity has been emphasized by the very recent observation[13] that such substitutions were more than 10^3 times more rapid in the open site of the recently discovered[13,14] [Sec-CH_3]-Co(*rac*-(*N*)-Me_6[14]dieneN$_4$)$(OH_2)CH_3^{2+}$ isomer than in the congested site of the [Pri-CH_3]-*racemic* isomer. Since water exchange rates (k_w) are not complicated by differences in reactant and product stability and since the anation rates are expected to be proportional to the water exchange rates in dissociative limits, our observations on the aquo–methyl complexes suggest that substitution rates in stereochemically complicated complexes such as Co^{III}(Me_6[14]diene)XY may involve some unusual kinetic feature superimposed on more apparent energetic factors (such as the differences in ground-state and intermediate-state strain energy).

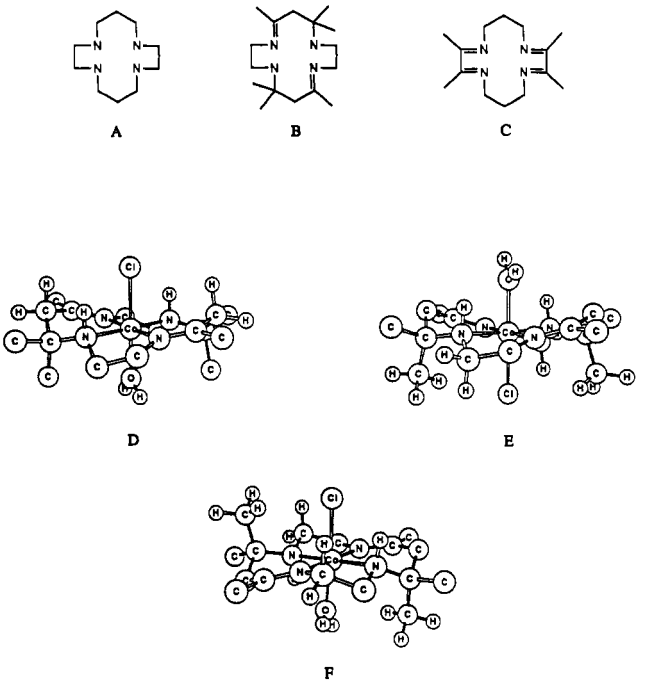

Figure 1. Skeletal structures of several macrocyclic ligands and graphics models of the Co(Me_6[14]dieneN$_4$)$(OH_2)Cl^{2+}$ isomers. A few of the hydrogens have been inserted to illustrate the stereochemical congestion near the coordinated chloride in the graphics models. The structures and models are as follows: [14]aneN$_4$, A; Me_6[14]dieneN$_4$, B; Me_4[14]tetraeneN$_4$, C; [Pri-Cl]–Co(*rac*-(*N*)-Me_6[14]dieneN$_4$)$(OH_2)Cl^{2+}$, D; [Sec-Cl]-Co(*rac*-(*N*)-Me_6[14]dieneN$_4$)$(OH_2)Cl^{2+}$, E; Co(*ms*-(*N*)-Me_6-[14]dieneN$_4$)$(OH_2)Cl^{2+}$, F.

The very different stereochemical congestion of the axial coordination sites of *trans*-Co^{III}(*rac*-(*N*)-Me_6[14]dieneN$_4$)X_2 complexes, one open and the other congested by neighboring equatorial ligand functional groups (see Figure 1), provide an unusually clear opportunity for examining the relative importance of thermodynamic and purely kinetic factors in determining reaction rates. We have used NMR techniques to determine the isomeric distributions that result from hydrolysis of *trans*-Co(*rac*-(*N*)-Me_6-[14]dieneN$_4$)Cl_2^+, and to monitor the subsequent hydrolysis, isomerization, etc. reactions. We have complemented these experimental observations with calculations of strain energy and changes of interatomic positions in the 5-coordinate macrocyclic ligand–cobalt(III) fragment using a modified MM2 program. The calculations simulate the changes within the complex fragment along a dissociative reaction coordinate. The observations provide very strong support for an interchange mechanism for substitution at Co(III) even when the nonlabile ligands are macrocyclic. Many of the allegedly mechanistic features inferred from previous studies very likely originate from the uncompensated diffrerences in complex stabilities.

Experimental Section

A. Preparation of Compounds. The following complexes were prepared by using literature procedures:[11] Me_6[14]dieneN$_4$·2HClO$_4$, [Co(Me_6[14]dieneN$_4$)$(OH_2)_2$](ClO$_4$)$_3$,[15,16] [Co(Me_6[14]dieneN$_4$)Cl_2]-ClO$_4$,[17,18] [Co(Me_6[14]dieneN$_4$)Br_2]ClO$_4$,[17,18] [Co(Me_6[14]dien-

(7) Hay, R. W.; Norman, P. R.; House, D. A.; Poon, C.-K. *Inorg. Chem.* **1965**, *4*, 1102.
(8) Hung, Y.; Busch, D. H. *J. Am. Chem. Soc.* **1977**, *99*, 4977.
(9) Johnson, D. W.; Brubaker, G. R. *Inorg. Chim. Acta* **1986**, *119*, 131.
(10) In our nomenclature, these axially different isomers could be labeled [Pri-Cl] and [Sec-Cl], respectively.[11]
(11) Ligand abbreviations: [14]aneN$_4$ = 1,4,8,11-tetraazacyclotetradecane; Me_4[14]tetraeneN$_4$ = 2,3,9,10-tetramethyl-1,4,8,11-tetraazacyclotetradeca-1,3,8,10-tetraene; *ms*-(*N*)-Me_6[14]dieneN$_4$ = *meso*-(*1,8*)-5,7,7,12,14,14-hexamethyl-1,4,8,11-tetraazacyclotetradeca-4,11-diene; *rac*-(*N*)-Me_6[14]dieneN$_4$ = *rac*-(*1,8*)-5,7,7,12,14,14-hexamethyl-1,4,8,11-tetraazacyclotetradeca-4,11-diene. The abbreviation Me_6-[14]dieneN$_4$ is used to include all conformational complexes or cases when the conformational stereochemistry is not pertinent. The prefixes [Pri-Cl] and [Sec-Cl] are used to refer to complexes with Cl^- in the "open" and stereochemically congested sites, respectively, in complexes containing the Me_6[14]dieneN$_4$ ligand in the racemic conformation; the designations [Pri] and [Sec] refer to the respective sites in the *rac*-(*N*)-Me_6[14]dieneN$_4$ complexes.
(12) Burkert, U.; Allinger, N. L. *Molecular Mechanics*; ACS Monograph 177; American Chemical Society: Washington, DC, 1982.
(13) Endicott, J. F.; Kumar, K.; Schwartz, C. L.; Lin, W.-K.; Perkovic, M. W. *J. Am. Chem. Soc.*, in press.
(14) Szalda, D. J. Work in progress. Creutz, C. Private communication.
(15) Durham, B. Ph.D. Dissertation, Wayne State University, 1979.
(16) Rillema, D. P.; Endicott, J. F.; Papaconstaninou, E. *Inorg. Chem.* **1971**, *10*, 1739.
(17) Poon, C. K.; Lee, W. K. *J. Chem. Soc., Dalton Trans.* **1974**, 2423.

Table I. Elemental Analyses of Selected Complexes

compd	% found (% theoret)			
	C	H	N	C/N
[[Pri-Cl]-Co(Me_6[14]dieneN$_4$)(OH_2)Cl](ClO_4)$_2$	33.45	6.15	9.81	3.41
	(33.50)	(6.30)	(9.80)	(3.42)
[Co(*ms*-(*N*)-Me_6[14]dieneN$_4$)Cl_2]ClO_4·1.5H_2O	35.53	6.41	10.42	3.41
	(35.80)	(6.57)	(10.44)	(3.43)
[Co(Me_6[14]dieneN$_4$)(NCS)Cl]ClO_4	38.08	6.18	13.04	2.92
	(38.35)	(6.06)	(13.16)	(2.91)
[Co(*ms*-(*N*)-Me_6[14]dieneN$_4$)(NCS)Cl]ClO_4·0.5H_2O	37.31	6.06	13.02	2.87
	(37.72)	(6.14)	(12.94)	(2.91)
[Co(Me_6[14]dieneN$_4$)Cl_2]ClO_4	37.69	6.42	10.95	3.44
	(37.70)	(6.33)	(11.00)	(3.43)

eN$_4$)(N_3)$_2$]ClO_4,[18] [Co(Me_6[14]dieneN$_4$)(N_3)Br]ClO_4,[17] [Co(Me_6[14]-dieneN$_4$)(OH_2)Cl](ClO_4)$_2$,[18] [Co(Me_6[14]dieneN$_4$)(OH_2)Br](ClO_4)$_2$,[18] [Co(Me_6[14]dieneN$_4$)(OH_2)N_3](ClO_4)$_2$,[18,19] and [Co(Me_6[14]dien-eN$_4$)(NCS)Cl](ClO_4).[18] Although the meso isomer of [Co(Me_6[14]-dieneN$_4$)Cl_2]ClO_4 can be prepared isomerically pure from $CoCO_3$ and the perchlorate salt of the protonated ligand, as reported previously,[18] the racemic isomer is always found in an isomeric mixture resulting from the reaction of cobaltous acetate with the macrocyclic ligand. The racemic isomer is slightly less soluble in methanol than is the meso isomer. Repeated extractions of the mixed solid with methanol yielded a mixture whose composition was constant at a ratio of 62% racemic to 38% meso isomer as determined by NMR spectra recorded in acetone-d_6 with TMS as a reference. Further extractions with methanol/ethanol (1:1 v/v and 1:2 v/v), methanol/isopropanol (1:1 v/v), and acetone resulted in an 80%/20% mixture of the racemic and meso isomers. The chemical shifts of the methyl groups in the meso and racemic isomers, respectively, were as follows: axial–geminal, 1.406 and 1.323 ppm; equatorial–geminal, 1.685 and 1.694 ppm; immine, 2.696 (triplet) and 2.719 (center of doublet) ppm. All peaks were referenced to acetone-d_6 (2.04 ppm) at room temperature.

The elemental analyses were performed by Midwest Microlab, Indianapolis, IN, or Central Instrumentation Facility, Wayne State University, Detroit, MI. Samples were analyzed for C, H, and N. The results are summarized in Table I. Figure 1 illustrates the ligands and isomers used in this study. *Warning!* The perchlorate salts prepared in this study are potentially explosive and should be handled with care.

B. Instrumental Techniques. 1. Nuclear Magnetic Resonance Spectroscopy. The ^{1}H spectra were determined by using a Nicolet NT 300 MHz spectrometer equipped with a Nicolet 1280 computer and a variable-temperature unit that used either N_2 or air. Some spectra were also recorded with a General Electric QE-300- or GN-300-MHz spectrometer. Deconvolution and calculation of full width at half-height and areas under each peak were carried out by using CAP (curve analysis program). Concentrations were based on the areas of the deconvoluted peaks. A few spectra of hydrolyzing Co(Me_6[14]dieneN$_4$)Cl_2^+ complexes were determined at Brookhaven National Laboratory by using a Bruker AM-300 spectrometer. Spectra were recorded at 25 °C unless otherwise indicated.

2. UV–Visible Spectroscopy. The spectra were recorded on a Cary 14 recording spectrophotometer by using either 1.0- or 10.0-cm quartz cells. Solvent was varied according to need.

3. Infrared Spectroscopy. The spectra were recorded on a Nicolet 20DX fourier transform spectrometer or on a Perkin-Elmer 283B double-beam infrared spectrometer. The solid samples were obtained as potassium bromide pellets.

C. Molecular Mechanics Calculations. MM-2 calculations were performed on the VAX 11/750 computer using the program MM2/MMP2 (Quantum Chemistry Program Exchange).[20] The original program by N. L. Allinger (University of Georgia) has been modified by Dr. Wang-Kan Lin (Ohio State University) to accommodate 6-coordinate metal ions. Minimized coordinates were transferred to a Macintosh computer by means of a reformatting program, MM2MAC by Marc W. Perkovic (Wayne State University). Graphic models could then be drawn by use of MODEL, a program provided by Professor H. B. Schlegel (Wayne State University). This program was also used to determine bond lengths and angles in calculated structures. The initial atomic coordinates used in the calculations were based on those previously obtained from minimization calculation of the Co(*rac*-(*N*)-Me_6[14]dien-eN$_4$)(OH_2)CH_3^{2+} and Co(*meso*-(N)-Me_6[14]dieneN$_4$)(OH_2)CH_3^{2+}.[11] The calculations for these complexes were originally based on coordinates obtained from X-ray crystal structures of the Co(*rac*-(*N*)-Me_6[14]dien-eN$_4$)(OH_2)CH_3^{2+} [20] and Co(*meso*-(*N*)-Me_6[14]dieneN$_4$)$(OH_2)_2^{2+}$,[22] respectively. The methyl–aquo complexes were then converted to chloro–aquo complexes by simple changes in atom type designation. The total energy of a molecule with a given set of atomic coordinates is based on the sum of individual interatomic interactions (comp = compression; di = dipole; tor = torsion):

$$E_{tot} = E_{comp} + E_{bend} + E_{VDW} + E_{di/di} + E_{tor} \quad (1)$$

These interaction energies were defined as in the Allinger–Yuh program,[20] and program parameters were employed for all interactions not involving the central metal. Values of parameters for interactions involving the metal were based on literature values[23] or reported vibrational frequencies. Torsion constants around the metal were assumed to be zero. Metal–ligand dipole moments were estimated from optical electronegativities.[24] A typical parameter set is included in the supplementary material (see paragraph at the end of this paper for ordering information). The calculational strategy was designed to evaluate changes in steric energy (ΔE_s) within the residual Co(N$_4$)X moiety as the leaving group was removed. To this end all the contributions to E_{comp}, E_{bend}, $E_{di/di}$, and E_{tor} that resulted from interactions of the leaving group were subtracted after the structure was minimized. Contributions of E_{VDW} were retained, since these should contribute to the reaction coordinate.

D. Kinetic Techniques. Solutions were prepared with D_2O (98% purchased from Aldrich Chemical Co.) or H_2O distilled in a Corning Mega-Pure still. The feed stock for the still was pretreated with a Corning 3508-A ultrahigh-purity demineralizer.

Solutions of oxygen-sensitive reactants were prepared in a nitrogen atmosphere and were mixed and transferred by using syringes and teflon tubing. Nitrogen was scrubbed of residual oxygen by passage through a column containing De-ox deoxygenation catalyst pellets. Samples of light-sensitive materials were prepared and transferred to instruments in dim light. Rapid reactions ($t_{1/2}$ < 10 min) were followed on the Cary 14 spectrometer. Slower reactions were monitored by NMR spectroscopy on the NT-300 or the GN-300 spectrometer.

The experimental NMR parameters were set up with a dummy sample before each day's run, in order to reduce the time for the initial time measurement. Timing was started at mixing, and samples were quickly transferred to NMR tubes and into the spectrometer. Reactions were monitored at intervals. NMR peaks were analyzed for relative area and position. DSS (3-(trimethylsilyl)-1-propanesulfonic acid, sodium salt hydrate) was added as a reference after the reaction was completed, so that reference peaks would not overlap sample peaks. First-order rate constants were obtained from the slopes of ln $[C_\infty - C_t]$ vs time plots.

Fast reactions were initiated by mixing the reactants in a spectrophotometer cell using a glass syringe fitted with a platinum needle to inject solutions through a rubber septum. Absorbance was monitored at a single wavelength, and plots of log (absorbance change) vs time were used to determine pseudo-first-order rate constants. The rate constant

(18) Sadasivan, N.; Kernohan, J. A.; Endicott, J. F. *Inorg. Chem.* **1967**, *6*, 770.
(19) Hay, R. W.; Lawrence, G. A.; Curtis, N. F. *J. Chem. Soc., Perkin Trans. 1* **1975**, 591.
(20) Allinger, N. L.; Yuh, Y. H. "QCPE 395 Molecular Mechanics; Operating Instructions for MM2 and MMP2 Programs 1977 Force Field", Quantum Chemistry Program Exchange, QCPE Program No. 395, Chemistry Department, Indiana University, Bloomington, IN.
(21) Heeg, M. J.; Endicott, J. F.; Glick, M. D. *Inorg. Chem.* **1981**, *20*, 1196.
(22) Endicott, J. F.; Lilie, J.; Kuszaj, J. M.; Ramaswamy, B. S.; Schmonsees, W. G.; Simic, M. G.; Glick, M. D.; Rillema, D. P. *J. Am. Chem. Soc.* **1977**, *99*, 429.
(23) Brubaker, G. R.; Johnson, D. W. *Coord. Chem. Rev.* **1984**, *53*, 1.
(24) Lever, A. B. P. *Inorganic Electronic Spectroscopy*, 2nd ed.; Elsevier: Amsterdam, 1984.

Table II. Vibrational Frequencies of $[Co(Me_6[14]dieneN_4)XY](ClO_4)_n$ Complexes[a]

complex	ν(O—H)	ν(N—H)	ν(C=N)	$\rho_r(CH_2)$	π(N—H)
$Co(ms\text{-}(N)\text{-}Me_6[14]dieneN_4)(Cl)_2^+$	3433 b, s	3185 s 3213 w	1654 s	777 m	847 w, 828 w
$Co(ms\text{-}(N)\text{-}Me_6[14]dieneN_4)(Br)_2^+$		3186 s 3179 w	1657 s	773 m	845 m, 826 w
$Co(rac\text{-}(N)\text{-}Me_6[14]dieneN_4)(OH_2)Cl^{2+}$	3500 b, s	3209 s 3183 w	1652 s	777 m	846 w, 828 m
$Co(rac\text{-}(N)\text{-}Me_6[14]dieneN_4)(OH_2)Br^{2+}$	3489 b, s	3203 s	1650 s	777 m	842 w, 825 m

[a] Spectrum run in KBr pellets; all values in cm^{-1}. Abbreviations: ν, stretch; ρ_r, rocking; π, out-of-plane bending; b, broad; s, strong; m, medium; w, weak. n = 1 or 2.

Table III. Equilibrium Concentrations and Constants for $Co(rac\text{-}(N)\text{-}Me_6[14]dieneN_4)(OH_2)Cl^{2+}$ in Varying Concentrations of HSO_3CF_3

$[H^+]$, M	$[P]_{eq}$,[a] M	$[M]_{eq}$,[b] M	$[R]_{eq}$,[c] M	K_{h2}^{P},[d] M	$K_{R,M}(H_2O,H_2O)$[e]	$K_{h2}^{P,M}$,[f] M
D_2O	9.0×10^{-4}	2.9×10^{-3}	1.2×10^{-4}	3.9×10^{-4}	24	9.4×10^{-3}
0.025	6.2×10^{-4}	2.3×10^{-3}	2.8×10^{-4}	1.2×10^{-3}	8	9.6×10^{-3}
0.1	2.9×10^{-4}	3.5×10^{-3}	1.6×10^{-4}	4.3×10^{-3}	11	4.7×10^{-2}
0.25	2.8×10^{-4}	2.8×10^{-3}	1.9×10^{-4}	2.1×10^{-3}	10	3.1×10^{-2}
0.5	8.4×10^{-5}	1.3×10^{-3}	9.6×10^{-5}	1.7×10^{-3}	14	2.3×10^{-2}
1.0	2.8×10^{-4}	2.6×10^{-3}	1.9×10^{-4}	1.9×10^{-3}	13	2.5×10^{-2}

[a] P = [Pri-Cl]-$Co(rac\text{-}(N)\text{-}Me_6[14]dieneN_4)(OH_2)Cl^{2+}$. [b] M = $Co(ms\text{-}(N)\text{-}Me_6[14]dieneN_4)(OH_2)_2^{3+}$. [c] R = $Co(rac\text{-}(N)\text{-}Me_6[14]dieneN_4)(OH_2)_2^{3+}$. [d] $K_{h2}^{P} = [R][Cl^-]/[P]$. [e] $K_{R,M}(H_2O,H_2O) = [M]/[R]$. [f] $K_{h2}^{P,M} = [M][Cl^-]/[P]$.

for substitution was obtained from plots of observed pseudo-first-order rate constants vs excess reagent. Ionic strength was maintained at 1.0 M with $NaCF_3SO_3$, and $[H^+]$ was between 0.1 and 10^{-2} M.

Results

A. Characterization of Isomers. All these complexes have the macrocycle in a nearly equatorial plane and the two monodentate ligands axial. The macrocyclic ligands have been useful in the kinetic studies because equivalent methyl groups appear as single peaks in the NMR spectra. Every isomer and energy change of axial ligands results in a unique spectrum. The $Me_6[14]dieneN_4$ complexes fall into two different stereochemical groups, depending on the coordinate conformation of the macrocyclic ligand. When the two amine protons are on the same side of the N_4 plane, both axial methyl groups, of the geminal methyl pairs, are on the side opposite to the NH protons. The resulting complexes are *d,l* racemates. For example, the $[trans\text{-}Co(Me_6[14]dieneN_4)(OH_2)Cl]X_2$ salts are isolated with the ligand in the racemic conformation.

When the amine protons are on opposite sides of the N_4 plane, the axial geminal methyl groups are also on opposite sides of the molecule and meso isomers result. We have found that complexes with identical axial ligands are most easily isolated with the ligand in the meso conformation.

The interconversion between the racemic and meso conformations of the $Me_6[14]dieneN_4$ ligand in these complexes is slow in acidic solutions, and complexes with the ligand in the less stable conformation can sometimes be isolated in strongly acidic solution. Thus, the racemic Co(II) complex has been prepared by reduction of a racemic starting material in 1 M acid. The product was originally characterized by infrared spectroscopy and by using NMR spectroscopy to identify its oxidation products.[25] X-ray crystal structure determination has shown the complex to be the 5-coordinate $[Pri\text{-}H_2O]\text{-}Co(rac\text{-}(N)\text{-}Me_6[14]dieneN_4)OH_2^{2+}$ species.[26]

The infrared absorption frequencies and band assignments are given in Table II for some meso (*ms*) and racemic (*rac*) complexes of the $Me_6[14]dieneN_4$ ligand. These spectra were used to distinguish the *rac* and *ms* isomers. Assignments of isomeric structures were made so as to be internally consistent with the NMR data and were ultimately referenced to the known structures of the diaquo and dichloro complexes.

B. Substitution Studies. Most of our studies were of the substitution and isomerization processes in the $Me_6[14]dieneN_4$ complexes, but a few studies were also performed with the related $Me_4[14]tetraeneN_4$ complexes.[25]

The NMR resonances from the three pairs of degenerate methyl groups of the $Me_6[14]dieneN_4$ complexes were well separated, the imine methyl peak being furthest downfield, the equatorial geminal methyl peaks being about 320 Hz upfield from the imine peaks, and the axial geminal methyl peaks about 170 Hz upfield from the equatorial peaks. There was no peak splittings due to environmental effects, and most of the species detected exhibited only a single peak in each region (the dichloro complexes were exceptions). The axial region usually gave the best peak separations for the different species in solution. The imine peaks were also reasonably well separated, but there was often appreciable overlap in the equatorial methyl region. Rate and equilibrium constants were based on the percentage areas of peaks in the axial methyl region. The reactions were followed in acidic (HSO_3CF_3, except where noted otherwise) D_2O solutions at 25 °C. In most cases the reactions were followed until there were not further changes in NMR peak intensities. The growth and decay of the various species were usually well fit by a single exponential dependence on time; in a few instances biexponential fits had to be employed.

Dissolution of the $Co(Me_6[14]dieneN_4)Cl_2^+$ in D_2O (acidic or neutral) resulted in solutions in which we detected (at the time of the initial NMR spectrum, ≥4 min) mostly aquo–chloro species, very small amounts of diaquo complexes, and no dichloro complexes (unless $[Cl^-] \gg 1$ M). We found three such aquo–chloro complexes: $[Pri\text{-}Cl]\text{-}Co(rac\text{-}(N)\text{-}Me_6[14]dieneN_4)(OH_2)Cl^{2+}$, which had been prepared and characterized separately; $Co(ms\text{-}(N)\text{-}Me_6[14]dieneN_4)(OH_2)Cl_2^+$, which was also obtained as the initial hydrolysis product of $Co(ms\text{-}(N)\text{-}Me_6[14]dieneN_4)Cl_2^+$; a new, less stable species, which we identify as $[Sec\text{-}Cl]\text{-}Co(rac\text{-}(N)\text{-}Me_6[14]dieneN_4)(OH_2)Cl^{2+}$. The equilibration of these solutions to a mixture of (predominantly) $[Pri\text{-}Cl]\text{-}Co(rac\text{-}(N)\text{-}Me_6[14]dieneN_4)(OH_2)Cl^{2+}$ and $Co(ms\text{-}(N)\text{-}Me_6[14]dieneN_4)(OH_2)_2^{2+}$ (typically in the ratio of 20:74, but depending on $[Cl^-]$) took from 17 h to 4 days depending on acidity ($10^{-3} \le [H^+]/M \le 0.5$). These subsequent reactions were slow enough that extrapolation of the initial rates back to the mixing time was possible, and by this means we estimate that the initial aquation of $Co(rac\text{-}(N)\text{-}Me_6[14]dieneN_4)Cl_2^+$ resulted in [Pri-Cl]:[Sec-Cl] racemic chloro–aquo isomer ratios that varied from 3:2 to 2:3 with large uncertainties arising from the poor signal-to-noise which resulted when the number of accumulations was reduced (typically to about 8) in order to obtain initial time information. This range of ratios is probably a good measure of the uncertainties in de-

(25) Schwarz, C. L. Ph.D. Dissertation, Wayne State University, 1988.
(26) Szalda, D. J.; Schwarz, C. L.; Endicott, J. F.; Fujita, E.; Creutz, C. *Inorg. Chem.* **1989**, *28*, 3214.
(27) Poon, C.-K.; Pun, D.-C. *Inorg. Chem.* **1980**, *19*, 568.

Table IV. Chemical Shifts of Methyl Peaks in $Co(Me_6[14]dieneN_4)XY^{n+}$ Complexes[a]

complex	δ(imine), ppm	δ(axial), ppm
$Co(ms\text{-}(N)\text{-}Me_6[14]dieneN_4)Cl_2^+$	2.696 ± 0.005[b,c]	1.406 ± 0.005[b]
$Co(rac\text{-}(N)\text{-}Me_6[14]dieneN_4)Cl_2^+$	2.719 ± 0.005[b,d]	1.323 ± 0.005[b]
[Sec-Cl]-$Co(rac\text{-}(N)\text{-}Me_6[14]dieneN_4)(OH_2)Cl^{2+}$	2.750 ± 0.003	1.234 ± 0.001
[Pri-Cl]-$Co(rac\text{-}(N)\text{-}Me_6[14]dieneN_4)(OH_2)Cl^{2+}$	2.716 ± 0.004	1.145 ± 0.002
$Co(ms\text{-}(N)\text{-}Me_6[14]dieneN_4)(OH_2)Cl^{2+}$	2.733 ± 0.003	1.092 ± 0.001
$Co(ms\text{-}(N)\text{-}Me_6[14]dieneN_4)(OH_2)_2^{3+}$	2.847 ± 0.003	1.125 ± 0.001
$Co(rac\text{-}(N)\text{-}Me_6[14]dieneN_4)(OH_2)_2^{3+}$	2.878 ± 0.007	1.079 ± 0.004

[a] Chemical shift values for runs at 0.001, 0.01, and 0.0235 M HO_3SCF_3 are averaged. All values referenced to DSS at 25 °C. [b] In acetone-d_6. [c] Triplet. [d] Center of doublet.

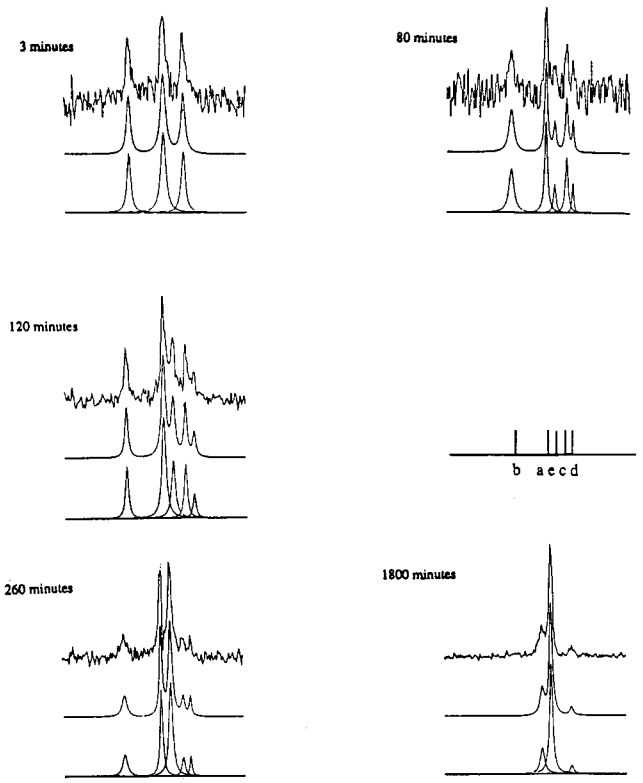

Figure 2. ^1H NMR spectra of a solution formed by dissolving a 62% racemic, 38% meso mixture of $[Co(Me_6[14]4,11\text{-}dieneN_4)Cl_2](ClO_4)$ isomers of 0.1 M HO_3SCF_3/D_2O at 25 °C. CAP simulations and peak resolutions are indicated under each spectrum. The observed peaks are assigned to the aquo–chloro and diaquo species as follows: a, [Pri-Cl]-$Co(rac\text{-}(N)\text{-}Me_6[14]dieneN_4)(OH_2)Cl^{2+}$; b, [Sec-Cl]-$Co(rac\text{-}(N)\text{-}Me_6[14]dieneN_4)(OH_2)Cl^{2+}$; c, $Co(ms\text{-}(N)\text{-}Me_6[14]dieneN_4)(OH_2)Cl^{2+}$; d, $Co(rac\text{-}(N)\text{-}Me_6[14]dieneN_4)(OH_2)_2^{3+}$; e, $Co(ms\text{-}(N)\text{-}Me_6[14]dieneN_4)(OH_2)_2^{3+}$.

termining peak intensities, and we will treat the chloro–aquo product ratio as approximately 1:1. An example of the resolved spectra (axial geminal methyl region) is shown in Figure 2. The averaged peak assignments for the pertinent species can be found in Table IV.

In principle, equilibrium constants can be calculated from the NMR peak ratios obtained in solutions at equilibrium or from the ratios of the rates of approach to equilibrium from different initial concentrations of diaquo, chloro–aquo, or dichloro species. In practice both approaches were limited in their usefulness by the mechanistic complexity of the reacting systems, by the solubilities of some species, and by the sensitivity of the NMR technique. We estimate that the threshold concentration for detection of these complexes, based on pairwise degenerate methyl group singlets, was approximately 10^{-5} M for our general operating conditions. On the basis of this limit, we estimate $K_{hl}^P \geq 0.1$ M.

$$Co(rac\text{-}(N)\text{-}Me_6[14]dieneN_4)Cl_2^+ \rightleftharpoons [Pri\text{-}Cl]\text{-}Co(rac\text{-}(N)\text{-}Me_6[14]dieneN_4)(OH_2)Cl^{2+} + Cl^- \quad K_{hl}^P$$

Since no [Sec-Cl]-$Co(rac\text{-}(N)\text{-}Me_6[14]dieneN_4)(OH_2)Cl^{2+}$ could be detected in the equilibrated mixtures, we can estimate $K_{P,S}(Cl,OH_2) \leq 0.01$ for

$$[Pri\text{-}Cl]\text{-}Co(rac\text{-}(N)\text{-}Me_6[14]dieneN_4)(OH_2)Cl^{2+} \rightleftharpoons [Sec\text{-}Cl]\text{-}Co(rac\text{-}(N)\text{-}Me_6[14]dieneN_4)(OH_2)Cl^{2+} \quad K_{P,S}(Cl,OH_2)$$

and $K_{hl}^S \geq 10^{-3}$ M for

$$Co(rac\text{-}(N)\text{-}Me_6[14]dieneN_4)Cl_2^+ \rightleftharpoons [Sec\text{-}Cl]\text{-}Co(rac\text{-}(N)\text{-}Me_6[14]dieneN_4)(OH_2)Cl^{2+} + Cl^- \quad K_{hl}^S$$

Finally, $K_{hl}^M \geq 0.3$ M for

$$Co(ms\text{-}(N)\text{-}Me_6[14]dieneN_4)Cl_2^+ \rightleftharpoons Co(ms\text{-}(N)\text{-}Me_6[14]dieneN_4)(OH_2)Cl^{2+} + Cl^- \quad K_{hl}^M$$

The rates of hydrolyses of the $Co(Me_6[14]dieneN_4)(OH_2)Cl^{2+}$ complexes were slow enough that they could be followed by using the NMR technique. However, these reactions were very complex. This complexity prohibited the ready resolution of the hydrolysis rate constants (k_{h2}) of the aquo–chloro complexes. Consequently, we were unable to establish whether there was a significant difference in the second hydrolysis rates of the [Pri-Cl] and [Sec-Cl] racemic isomers.

The issue of thermodynamic contributions to hydrolysis rates does not arise in water exchange reactions since $K_{ex} = 1.0$. If anation and water exchange reactions both occurred by dissociative pathways (D or I_D) that involved very short-lived intermediates and very similar Co–OH_2 bond extension in the transition state for substitution (r_{TS}), then water exchange rate constants (k_w) could be inferred from anation rate constants (k_{an}) by using[2-4]

$$k_{an} \approx K_0 k_w \qquad (2)$$

where K_0 is the ion pair association constant. For this reason we have examined the anation reactions of several $Co(N_4)(OH_2)Cl^{2+}$ complexes.

NMR spectra of mixtures of $Co(N_4)(OH_2)Cl^{2+}$ and NCS^- were complicated by the presence of many peaks corresponding to the decomposition and/or formation of different species throughout the reactions. An example of the spectrum obtained at an intermediate stage of such a reaction is shown in Figure 3. The reaction products were identified of reactions of [Pri-Cl]-$Co(rac\text{-}(N)\text{-}Me_6[14]dieneN_4)(OH_2)Cl^{2+}$ with thiocyanate for different concentrations of NaCl and HSO_3CF_3. The concentration of the NaSCN was kept low (approximately half the $[Co^{3+}]$), so the reaction would progress at slow rates and allow the accumulation of accurate NMR data. The decay of [Pri-Cl]-$Co(rac\text{-}(N)\text{-}Me_6[14]dieneN_4)(OH_2)Cl^{2+}$ was found to result from competitive aquation and anation reactions. For some conditions the anation was slightly faster than the aquation and the metastable chloro–thiocyanato product then rose to a maximum concentration and decayed into an aquo–thiocyanato species. Pseudo-first-order rate constants, based on starting material decay, were $[NCS^-]$ dependent, as shown in Figure 4. From the slope in Figure 5, $k_{an}^P = 3.4 \times 10^{-3}$ M^{-1} s^{-1}, and from the intercept, $k_b = 1.2 \times 10^{-5}$ s^{-1}. This value of k_b is in the range of values estimated for hydrolysis of [Pri-Cl]-$Co(rac\text{-}(N)\text{-}Me_6[14]dieneN_4)(OH_2)Cl^{2+}$ under similar conditions.

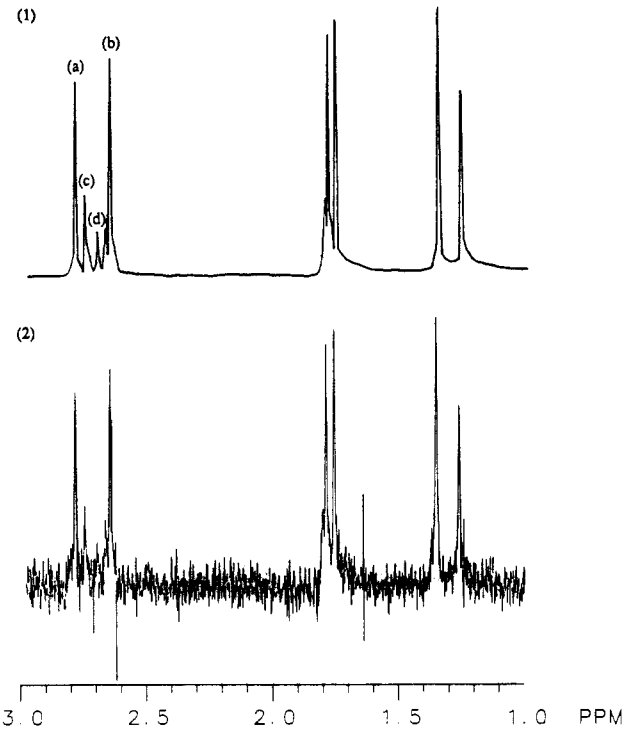

Figure 3. ^1H NMR spectra of the reaction of [Pri-Cl]-Co(*rac*-(*N*)-Me_6[14]dieneN$_4$)$(OH_2)Cl^{2+}$ with NCS^-. The reaction was run at total [Co(III)] = 2.4×10^{-3} M, [NaNCS] = 1.7×10^{-2} M, [NaNCS] = 1.7×10^{-2} M, [HSO_3CF_3] = 0.10 M, and [$NaSO_3CF_3$] = 0.50 M in D_2O at 25 °C. Spectrum 1 is a trace of spectrum 2, with noise repressed, in order to emphasize the peaks. Peak assignments: a, [Pri-Cl]-Co(*rac*-(*N*)-Me_6[14]dieneN$_4$)$(OH_2)Cl^{2+}$; b, Co(Me_6[14]dieneN$_4$)$(NCS)Cl^{2+}$; c, [Pri-NCS]-Co(*rac*-(*N*)-Me_6[14]dieneN$_4$)$(OH_2)NCS^{2+}$; d, Co(Me_6[14]-dieneN$_4$)$(NCS)_2^+$.

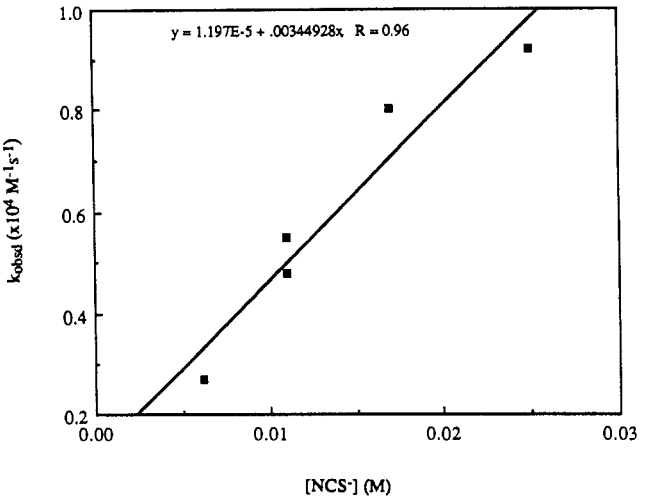

Figure 4. Plot of the pseudo-first-order rate constant k_{obsd} vs [NCS^-] for the reaction of [Pri-Cl]-Co(*rac*-(*N*)-Me_6[14]dieneN$_4$)$(OH_2)Cl^{2+}$ with NCS^-. Reactions were run at 25 °C in 0.5 M $NaSO_3CF_3$ (D_2O; 0.01 M HSO_3CF_3). Rates are based on NMR determinations of the decreases in concentration of the Co(III) starting material.

C. Molecular Mechanics Studies. Removal of an axial ligand (Y) from the sterically congested, [Sec], position of Co(*rac*-(*N*)-Me_6[14]dieneN$_4$)XY results in an appreciable relaxation of strain energy within the Co(MCL)X fragment. A smaller relaxation of strain energy is associated with the removal of a ligand from the open, [Pri], position. Calculated values of ΔE_s are summarized in Table V. These strain relaxation energies were spread over most of the components of E_{min}. Values of ΔE_s were independent of the Co–Y dipole moment.

The values of ΔE_s change over very substantial increases (>1.5 Å) in the Co–Cl bond length when the chloride is removed from the [Sec] position in Co(*rac*-(*N*)-Me_6[14]dieneN$_4$)Cl_2^+, as is illustrated in Figure 5. In contrast, the smallest value of ΔE_s is achieved when the chloride is removed only about 0.5 Å from the [Pri] site. The behavior of the Co(*ms*-(*N*)-Me_6[14]dieneN$_4$)Cl_2^+ complex is intermediate, with the energy of the Co(*ms*-(*N*)-Me_6[14]dieneN$_4$)Cl^{2+} reaching its smallest value for about a 1.25-Å increase in the Co–Cl bond length.

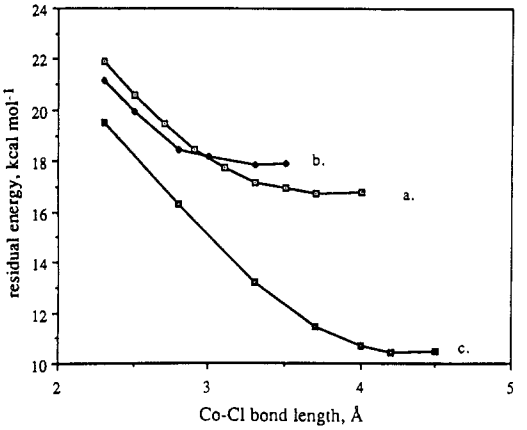

Figure 5. Plots of the residual Co(N_4)Cl strain energy, E_s, vs the distance between Co(III) and the leaving group for Co(Me_6[14]dieneN$_4$)Cl_2^+ complexes. The behavior of the meso isomer is shown in curve a. The behavior of the racemic isomer is shown in curve b, for removal of Cl from the [Pri] position, and curve c, for removal of Cl from the [Sec] position. Values of residual strain energies in the Co(N_4)Cl^{2+} fragment were determined from the MM2 minimizations (E_{tot}) for each Co–leaving group distance by removing all but the van der Waals interaction energies with the leaving group. In this particular data set the Co–leaving group dipoles were retained.

Table V. Summary of Molecular Mechanics Calculations for Co^{III}(Me_6[14]dieneN$_4$)XY Hydrolysis Reactions

conformational isomer	X	Y	leaving group	ΔE_s,[a] kcal mol^{-1}	ΔE(Cl,H_2O),[b] kcal mol^{-1}
racemic	Cl	Cl	Pri-Cl	3.3 ± 0.1	3.8
racemic	Cl	Cl	Sec-Cl	8.8 ± 0.2	6.0
[Pri-Cl]-racemic	H_2O	Cl	Pri-Cl	2.4 ± 0.1	
[Sec-Cl]-racemic	H_2O	Cl	Sec-Cl	7.4 ± 0.2	
[Pri-CH_3]-racemic[c]	CH_3	H_2O	Sec-H_2O	4.6 ± 0.1	0
[Sec-CH_3]-racemic[c]	CH_3	H_2O	Pri-H_2O	4.3 ± 0.1	0
meso	Cl	Cl	Cl	5.2 ± 0.1	5.5
meso	H_2O	Cl	Cl	4.2 ± 0.1	
meso[c]	CH_3	H_2O	H_2O	2.5 ± 0.1	0

[a] Differences in the residual Co(N_4)X energies calculated for the ground state and the limit for Co–Y dissociation. The dissociation limit was defined as the Co–Y bond length whose further extension did not change E_s. See Figure 5. Values are averaged over several values of the Co–Y bond length and calculations with and without Co–Y dipole moments. Non van der Waals contributions due to the leaving group (Y) interactions with the metal and with the macrocyclic ligand have been subtracted from the minimized energy to obtain the residual energies, E_s. [b] Differences in the calculated values of the minimized strain energies, E_{tot}, for the Co(Me_6[14]-dieneN$_4$)$(OH_2)X^{2+}$ and Co^{III}(Me_6[14]dieneN$_4$)XY ground states. [c] Calculations from ref 13.

Discussion

This study has established that the coordination site with the greatest stereochemical strain in a simple coordination complex, Co(*rac*-(*N*)-Me_6[14]dieneN$_4$)Cl_2^+, is not the most labile site for substitution. The pertinent issues and detailed analyses require some further comment.

A. Axial Ligand Hydrolysis in *trans*-Co(N_4)Cl_2^+ Complexes. We have qualitatively confirmed previous reports that the first step in the hydrolysis is complete within a few minutes for the Me_6[14]dieneN$_4$ and Me_4[14]tetraeneN$_4$ complexes.[6,17,18] However, the NMR technique has permitted a definitive analysis of the course of these substitution processes in acidic solution. Important features of these reactions are now evident that could not be inferred from changes in the broad visible (or ultraviolet) absorption bands used to characterize these reaction systems in

Table VI. Comparison of Thermodynamic and Kinetic Parameters in the Hydrolysis Reactions (at 25 °C) $Co^{III}(N_4)XY + H_2O \rightleftharpoons Co^{III}(N_4)(OH_2)X + Y$

macrocyclic ligand (N_4)	X	Y	leaving position	K(obsd),[a] M	K(calcd), M	k_{obsd}, s^{-1}
rac-(*N*)-Me_6[14]dieneN$_4$	Cl	Cl	Pri	≥ 10[c]	5×10^2[b]	2×10^{-2}[d]
rac-(*N*)-Me_6[14]dieneN$_4$	Cl	Cl	Sec	≥ 100[c] ($\geq 10^3$)[e]	2×10^4[b]	2×10^{-2}[d]
rac-(*N*)-Me_6[14]dieneN$_4$	Cl	H_2O	Sec	1.0[f]	1.0[f]	0.9×10^{-3}[g]
rac-(*N*)-Me_6[14]dieneN$_4$	CH_3	H_2O	Pri	1.0[f]	1.0[f]	$>10^4$[g,h]
rac-(*N*)-Me_6[14]dieneN$_4$	CH_3	H_2O	Sec	1.0[f]	1.0[f]	1.3[g,h]
ms-(*N*)-Me_6[14]dieneN$_4$	Cl	Cl	*i*	≥ 10	10^4[b]	3.6×10^{-2}[d]
ms-(*N*)-Me_6[14]dieneN$_4$	CH_3	H_2O	*i*	1.0[f]	1.0[f]	3.1[g,h]
Me_4[14]tetraeneN$_4$	Cl	Cl	*i*	5.5	~1[b,j]	2.1×10^{-2}[k]
Me_4[14]tetraeneN$_4$	Cl	OH_2	*i*	1.0[f]	1.0[f]	≤ 10[l]
Me_4[14]tetraeneN$_4$	OH_2	Cl	*i*	0.030[l]		
Me_4[14]tetraeneN$_4$	CH_3	OH_2	*i*	1.0[e]	1.0[f]	217[f,g]

[a] Based on NMR spectra of equilibrated mixtures as discussed in text. [b] Based on MM2 calculations of ground-state strain energies (E_{tot}): $-RT \ln K(\text{calcd}) = \Delta E_{tot}$. This calculated value neglects any contributions of solvation energy differences and entropy changes to k. Since the solvation energy differences of H_2O and Cl^- have been neglected, these four values of K(calcd) should be viewed as relative values. [c] Limit based on detection threshold for NMR spectra. [d] Based on a composite rate constant of 2.1×10^{-2} s^{-1}, reported in: Kernohan, J. A.; Endicott, J. F. *Inorg. Chem.* **1970**, *9*, 1504. [e] Based on the equilibrium distribution of isomers and the detection threshold for the preceding entry. [f] For water exchange. [g] $k_{obsd} = k_{an}/K_0$, where k_{an} was determined from NCS^- anation rates. [h] Reference 13. [i] Axially symmetric ligand. [j] Based on the very small (<1 kcal mol^{-1}) of ΔE_s found for Co(Me_4[14]tetraeneN$_4$)(OH_2)CH_3^{2+} complexes as the Co–OH_2 bond length was altered.[13] [k] Rillema, D. P.; Endicott, J. F.; Barber, J. R. *J. Am. Chem. Soc.* **1973**, *95*, 6987. [l] Schwarz, C. L. Ph.D. Dissertation, Wayne State University, 1988.

the earlier studies. While the previously reported acid hydrolysis rates are generally consistent with our observations, we find that the previous work has consistently overestimated the stabilities of the chloro complexes. The best current estimates of the rate and equilibrium data for the first hydrolysis step are collected in Table VI.

The hydrolytic equilibria of Co(*rac*-(*N*)-Me_6[14]dieneN$_4$)Cl_2^+ proved to be a considerable challenge to investigate. It is necessary to consider six different complexes in order to properly account for the observations on this system. The relationships between these species are indicated schematically in Figure 6. The equilibrium between the racemic and meso isomers involves inversion at a coordinated amine, and it is expected to be base catalyzed, in reasonable accord with our limited observations at high pH. This isomerization appears to be mediated by the diaquo species in solutions of high acidity; however, other pathways may contribute when $[H^+]$ is less than about 10^{-3} M. Our attempts to examine these equilibria in the presence of excess chloride were frustrated by the insolubility of the dichloro complex in the reaction medium, but the very limited observations suggest that the further aquation of [Sec-Cl]-Co(*rac*-(*N*)-Me_6[14]dieneN$_4$)(OH_2)Cl^{2+} is mediated by a relatively labile equilibrium with the dichloro complex, followed by substitution into the [Sec] position. On the basis of the minimized ground-state energies only, we would predict $K_{S,P}$(calcd) ≈ 45, whereas the NMR data give $K_{S,P}$(obsd) $\geq 10^2$. This is probably very good agreement, since $K_{S,P}$(calcd) is very sensitive to small changes in the MM2 input parameters (such as the difference between the Co–OH_2 and Co–Cl dipole moments; these were set equal to −1.0 and −1.1 D, respectively, in our calculation) and entropy differences have not been estimated. The MM2 calculations also ignore differences in hydration energies, although this should not be a major factor in $K_{S,P}$.

Clearly the chloride coordinated to the Sec position is the least stable, yet this site is not significantly labilized in the Co(*rac*-(*N*)-Me_6[14]dieneN$_4$)Cl_2^+ complex. The simplest resolution of this apparent paradox is that (a) substitution in this and probably most macrocyclic Co(III) complexes involves the interchange of entering and leaving groups, not a limiting dissociative mechanism, and (b) the macrocyclic ligand shelters the stereochemically congested coordination site from attack by the entering group until the departing ligand has moved an unusually great distance from the metal center; i.e., r_{TS} varies from complex to complex.

Conclusions

The hydrolysis of Co(*rac*-(*N*)-Me_6[14]dieneN$_4$)Cl_2^+ provides a very clear demonstration of the *kinetic* implications of an interchange mechanism of substitution. These are two possible sites for substitution, the stereochemically congested [Sec] and the open [Pri] sites. The stereochemical factors favor the isomer substituted

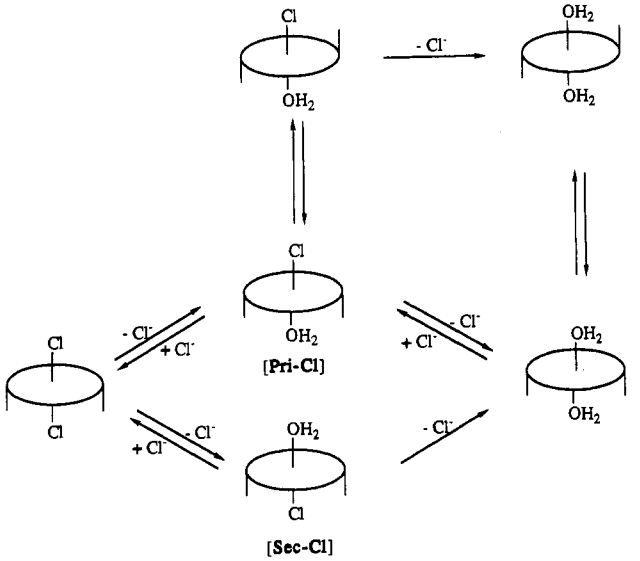

Figure 6. Scheme showing the interrelationships between isomers and complexes observed in the acid hydrolyses of Co(*rac*-(*N*)-Me_6[14]dieneN$_4$)Cl_2^+. For simplicity, only the axial geminal methyl groups are indicated on the macrocyclic ring. In principle racemic $\rightleftharpoons$ meso equilibria could involve any of the racemic complexes, and it is not clear which of the four possible isomerization equilibria is most facile. We have indicated the isomerization equilibria involving only the dominant solution species.

at the [Sec] site by a factor of more than 10^2 in the respective aquation equilibrium constants. Molecular mechanics calculations demonstrate that there is a similar ratio of stabilities in the 5-coordinate Co(N_4)Cl^{2+} isomers, with [Sec-Cl] being much less stable than [Pri-Cl]. These stability ratios would be directly reflected in the substitution rates for dissociative pathways (I_D or D, respectively), and such mechanisms would require that substitution be at least 100 times faster at the [Sec] than at the [Pri] site. Instead, the rates of substitution are comparable. Consequently, the substitution cannot be purely dissociative; there must be a significant associative component.

Our observations indicate that the analyses of substitutional processes in transition-metal complexes with macrocyclic ligands have often been based on incorrect mechanistic premises. As a result, many earlier inferences about the relationship between substitution rates and metal–ligand bond energies, cis vs trans interactions, electronic vs stereochemical effects, etc., need to be reexamined.

Acknowledgment. We are grateful to M. W. Perkovic for assistance with some of the calculations, to Professor H. B. Schlegel for providing us with access to the MODEL program, and to Dr. C. Creutz for providing us with pertinent information prior to publication. We are also grateful to the Chemistry Department at Brookhaven National Laboratory for allowing us to monitor a few reactions with their NMR spectrometer. The initial coordinates for the MM2 calculations were derived from those of the corresponding methyl-aquo complexes. These were initially set up by using The Ohio State University Chemistry Department's Image Center with a great deal of assistance from Dr. W.-K. Lin. We are very appreciative of this assistance. C.L.S. gratefully acknowledges partial support through a Graduate and Professional Opportunities Scholarship from the Department of Education.

Registry No. Co(*ms*-(*N*)-Me_6[14]dieneN$_4$)Cl_2^+, 55058-00-9; Co(*rac*-(*N*)-Me_6[14]dieneN$_4$)Cl_2^+, 122742-53-4; [Sec-Cl]-Co(*rac*-(*N*)-Me_6[14]dieneN$_4$)$(OH_2)Cl^{2+}$, 121701-57-3; [Pri-Cl]-Co(*rac*-(*N*)-Me_6-[14]dieneN$_4$)$(OH_2)Cl^{2+}$, 122742-54-5; Co(*ms*-(*N*)-Me_6[14]dieneN$_4$)-$(OH_2)Cl^{2+}$, 121701-57-3; NCS^-, 302-04-5.

Supplementary Material Available: A table listing a typical set of MM2 parameters for metal-ligand interactions (2 pages). Ordering information is given on any current masthead page.

Contribution from the Department of Physiological Chemistry, College of Medicine, The Ohio State University, Columbus, Ohio 43210, Corporate Research Science Laboratories, Exxon Research and Engineering Company, Annandale, New Jersey 08801, Department of Chemistry, University of Georgia, Athens, Georgia 30602, and National Synchrotron Light Source, Brookhaven National Laboratory, Upton, New York 11973

EXAFS Analysis of Xanthine Oxidase Complexes with Alloxanthine, Violapterin, and 6-Pteridylaldehyde[⊥]

R. Hille,[†] G. N. George,[‡] M. K. Eidsness,[§] and S. P. Cramer*,[∥]

Received September 9, 1988

The structure of the molybdenum site of xanthine oxidase in the complexes with alloxanthine, violapterin, and 6-pteridylaldehyde has been investigated by using X-ray absorption spectroscopy. The strongest component in the EXAFS spectrum is assigned to Mo-S bonds at 2.38 ± 0.03, 2.40 ± 0.03, and 2.46 ± 0.03 Å, respectively. In all cases, a second EXAFS component was identified as corresponding to a terminal oxo group with a bond length of 1.66-1.71 Å. A terminal sulfur ligand, with a Mo=S bond length of 2.20 ± 0.03 Å, was observed for the oxidized 6-pteridylaldehyde complex. However, the presence of a short Mo=S bond (≤2.30 Å) was ruled out for the alloxanthine and violapterin complexes. The EXAFS results are compared with previous proposals for the alloxanthine-xanthine oxidase complex.

Introduction

Xanthine oxidase (XO) is an enzyme containing molybdenum, FAD, and (2Fe-2S) clusters, which catalyzes the oxidations of hypoxanthine to xanthine and xanthine to uric acid, reactions that take place at the molybdenum center of the enzyme.[1] A variety of aromatic heterocycles form complexes at the molybdenum center that are of potential relevance to the catalytic cycle, as illustrated in Scheme I.

Alloxanthine (1*H*-pyrazolo[3,4-*d*]pyrimidine-4,6-diol) forms a tight complex with the Mo(IV) site of reduced xanthine oxidase.[2] This complex is of clinical importance because it is the inhibitory product of the reaction of xanthine oxidase with allopurinol (1*H*-pyrazolo[3,4-*d*]pyrimidin-4-ol) used in the treatment of hyperuricaemia.[3] The electron paramagnetic resonance (EPR) spectrum of the Mo(V)-alloxanthine complex with XO[4-6] is similar to the Very Rapid signal, which arises from a transient intermediate thought to be of catalytic significance[7,8] in the oxidation of xanthine and other substrates.[8,9] The similarity of the Mo(V) EPR signals suggests some degree of structural homology between the alloxanthine complex and the Very Rapid intermediate. Information about the alloxanthine complex is thus ultimately relevant to the catalytic mechanism of xanthine oxidase.

Violapterin (2,4,7-trihydroxypteridine) is the product of xanthine oxidase acting on the substrate lumazine (2,4-dihydroxypteridine) and forms a catalytically important complex with the reduced Mo(IV) enzyme.[10] This complex exhibits a long wavelength (650 nm) absorption band and is thought to correspond to a product complex (E_{red}·P) in the catalytic cycle. Davis et al. have labeled this a "charge-transfer" complex in which the molybdenum center of the enzyme is assigned as the donor and violapterin is assigned as the acceptor.[10] Pteridylaldehyde (2-amino-4-hydroxy-6-formylpteridine) forms a complex with a

Scheme I. Structures and Reactions of Xanthine Oxidase Substrates and Inhibitors

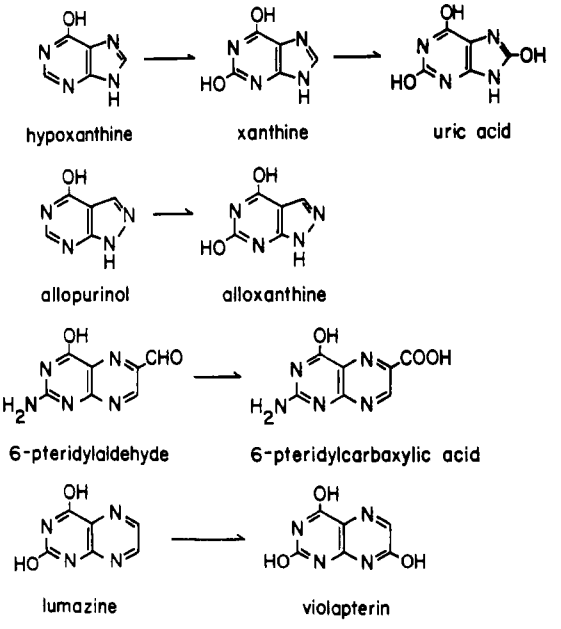

[†] The Ohio State University.
[‡] Exxon Research and Engineering Co.
[§] University of Georgia.
[∥] Brookhaven National Laboratory.
[⊥] Abbreviations: FAD, flavin adenine dinucleotide, XO, xanthine oxidase; XAS, X-ray absorption spectroscopy; EXAFS, extended X-ray absorption fine structure.

(1) Hille, R.; Massey, V. *Molybdenum Enzymes*; Spiro, T. G., Ed.; John Wiley: New York, 1985; pp 443-518.
(2) Massey, V.; Komi, H.; Palmer, G.; Elion, G. B. *J. Biol. Chem.* **1970**, *245*, 2837-2844.
(3) Wade, A., Ed. *Martindale: The Extra Pharmacopoeia*, 27th ed.; The Pharmaceutical Press: London, 1977; pp 371-372.
(4) Tanner, S. J. Ph.D. Thesis, University of Sussex, 1978.
(5) Williams, J. W.; Bray, R. C. *Biochem. J.* **1981**, *195*, 753-760.
(6) Hawkes, T. R.; George, G. N.; Bray, R. C. *Biochem. J.* **1984**, *218*, 961-968.

0020-1669/89/1328-4018$01.50/0